Supporting Material for

Physical determinants of β-barrel membrane protein folding in lipid vesicles

Alison H. Dewald, Jacqueline C. Hodges, and Linda Columbus

The supporting material consists of the materials and methods for Opa cloning, expression and purification and liposome preparation, three tables, and nine figures

MATERIALS AND METHODS

Cloning, expression, and purification. The opa_{60} and opa_{50} genes originally in pEX vectors were generously provided by Martine Bos (Utrecht University, The Netherlands) and were sub-cloned into the pET28b vector (EMD Chemicals, Gibbstown, NJ), which encodes a Thrombin cleavable N-terminal His_6-tag (MGSSHHHHHHSSGLVPRGSHM). For expression, the opa-containing plasmid was transformed into a BL21(DE3) *Escherichia coli* strain. Cell cultures were grown to an $OD_{600} \approx 0.8$ at 37 ^oC in Luria-Bertani medium supplemented with kanomyacin (50 µg/mL). Protein expression to inclusion bodies was induced overnight at the same temperature with 1 mM isopropyl-β-thio-D-galactoside. Opa_{60} and Opa_{50} sequences are shown in Supplementary Figure S1. When expressed natively in *Neisseria*, these proteins are named OpaI and OpaA, respectively (1) (see Table 1 in (2)). Cells from 1-L culture were harvested by centrifugation (5000g, 20 min, 12^{o}C), resuspended in 15 mL lysis buffer (50 mM tris, pH 8.0, 150 mM NaCl, 1 Complete protease inhibitor pellet (Roche)), and lysed using a microfluidizer (Microfluidics model 110L, Newton, Mass). The insoluble fraction was pelleted (12,000 x g, 30 min, 12^{o}C), washed by resuspension in lysis buffer, and then pelleted again. Opa protein was solubilized from inclusion bodies in 30 mL extraction buffer (lysis buffer with 8M urea) at room temperature with constant stirring overnight. The insoluble fraction was removed by centrifugation (12,000 x g, 30 min, 12^{o}C), and the supernatant was applied to cobalt chelating resin (GE Healthcare, Piscataway, NJ) previously equilibrated with extraction buffer. The column was washed with 15 column volumes of wash buffer (20 mM sodium phosphate, pH 7.8, 150 mM NaCl, 20 mM imidazole, 7.5 M urea) and the protein was eluted with five column volumes of elution buffer (20 mM sodium phosphate, pH 7.0, 150 mM NaCl, 680 mM imidazole, 7.5 M urea). The eluate was concentrated (MWCO = 10 kDa) to 15 mg/mL, with an expression yield of ≈25 mg (from 1 L of culture). Concentration was determined by measuring the absorbance at 280 nm. The predicted molar extinction coefficients, for Opa_{60} and Opa_{50}, each having N-terminal his-tags, are 41830 and 40340 $M^{-1}cm^{-1}$, respectively (3). Proteins were stored at room temperature, and for refolding experiments were used the next day.

Preparation of SUV Liposomes. Lipid stocks including 1-palmitoyl-2-oleoyl-*sn*-glycero-3-phosphocholine (POPC), 1-palmitoyl-2-oleoyl-*sn*-glycero-3-phospho-(1'-*rac*-glycerol) (POPG), 1,2-dioleoyl-*sn*-glycero-3-phosphocholine (DOPC), *E. coli* total extract, *E. coli* polar extract, 1,2-didecanoyl-*sn*-glycero-3-phosphocholine ($diC_{10}PC$), 1,2-dilauroyl-*sn*-glycero-3-phosphocholine ($diC_{12}PC$), 1,2-dimyristoyl-*sn*-glycero-3-phosphocholine ($diC_{14}PC$), 1,2-dipalmitoyl-*sn*-glycero-3-phosphocholine ($diC_{16}PC$), 1,2-distearoyl-*sn*-glycero-3-phosphocholine ($diC_{18}PC$), 1,2-didecanoyl-*sn*-glycero-3-phospho-(1'-*rac*-glycerol) (sodium salt) ($diC_{10}PG$), 1,2-dimyristoyl-*sn*-glycero-3-phospho-(1'-rac-glycerol) (sodium salt) ($diC_{14}PG$), 1,2-dimyristoleoyl-*sn*-glycero-3-phosphocholine ($diC_{14:1}PC$), and 1,2-dipalmitoleoyl-*sn*-glycero-3-phosphocholine ($diC_{16:1}PC$) were obtained from Avanti Polar Lipids (Alabaster, AL). Lipids, originally dissolved in chloroform, were dried under a stream of nitrogen, then, overnight in a vacuum desiccator to yield 60 µmol lipid. The lipid films were dispersed in 10 mM buffer (pH 7, bis-tris; pH 8, Tris; pH 9 and 10, glycine; pH 11 and 12, sodium borate) with 1 mM EDTA to a final lipid concentration of 6 mM. The lipid dispersions were sonicated for 35 min using a Heat Systems-Ultrasonics (Farmington, NY) microtip at 50% output, diluted with buffer to 2.4 mM, and then equilibrated overnight at 37^{o}C for use the following day. Lipids dispersions were visually clear following sonication, with vesicles 30-60 nm in diameter, (except for diC10:0PC vesicles which were ~130 nm diameter; see Table S1 in the Supporting Material) as measured by dynamic light

scattering (DynaPro Titan, Wyatt Technology Corp, Santa Barbara, CA). The larger size of the diC_{10}PC vesicles persisted following 20, 35, or even 55 minutes of sonication. The folding of Opa_{60} was also tested in vesicles of diC_{10}PC, diC_{12}PC, and diC_{14}PC created using Avanti Polar Lipids mini-extruder with a 50 nm pore membrane. The total fold, aggregate, and lipid fraction folded did not vary significantly for vesicles formed with the 50 nm pore size versus those created via sonication (data not shown). Thin layer chromatography (TLC) verified lipid purity but showed some lipid degradation at pH 12 (data not shown).

Gel Analysis with ImageJ Software. Gels were analyzed following the method at http://lukemiller.org/index.php/2010/11/analyzing-gels-and-western-blots-with-image-j/. Briefly, gel images were converted to 8-bit grayscale then inverted to give high expression bands higher numerical values when measured. Bands were selected and area, mean gray value, and integrated density (area x mean gray value) were recorded for each, including a standard (25 kDa band of Promega Broad Range Molecular Weight Marker) loaded onto each gel.

Fluorescence Spectroscopy. Fluorescence spectra were collected in a FluoroMax-3 spectrofluorometer (HORIBA JobinYvon, Edison, NJ). The excitation wavelength was 295 nm and Trp emission spectra of Opa proteins were collected over 305-475 nm at a scan rate of 0.15 nm/sec. The 4.2 nm slits were used for both excitation and emission. All samples contained 6 μM Opa protein, and all spectra were background-corrected with a proper reference sample of identical composition but without protein.

TABLE S1 Phosphocholine lipid vesicle size and polydispersity (Pd) measured by DLS

Carbon Chain	Radius (nm)	% Pd
10	64.4 ± 2.9	7.8 ± 2.3
12	26.0 ± 1.2	8.6 ± 3.6
14	20.9 ± 5.5	9.4 ± 2.5
16	29.7 ± 1.6	7.5 ± 6.1
18	25.3 ± 0.6	5.5 ± 5.1

TABLE S2 OmpA folding conditions applied to Opa_{60}

Year, Ref.	Optimized Folding Conditions		Folding Efficiency	
	Lipid, Temperature (^oC)	Buffer, pH	OmpA	Opa_{60}
1992, (4)	$diC_{14}PC$, 30	10 mM KP_i, 7.3	40-50%	<1%
1995, (5)	$diC_{14}PC$, 30	20 mM glycine, 10	>95%	<1%
1996, (6)	DOPC, 40	10 mM glycine, 150 mM NaCl, 1 mM EDTA, 8.3	>95%	<1%
2004, (7)	POPC or 92.5/7.5 POPC/POPG, 37.5	10 mM glycine, 2 mM EDTA, 10	>95%	<1%

TABLE S3 Hydrocarbon thickness of lipids

Lipid	Reported T_m* (^oC)	Measurement temperature (^oC)	Thickness of hydrocarbon region (Å)
diC10:0PC	-	20	18.5†
diC12:0PC	-1.8	20	22.5†
diC14:0PC	23	36	26.0†
diC16:0PC	42	44	29.0†
diC18:0PC	55	60	32.5†
diC14:1PC	-	30	23.4ǂ
diC16:1PC	-36	30	26.2ǂ
diC18:1PC	-20	30	29.0ǂ

* From Silvius (8)

† Phosphate-phosphate distance reported by Nagle *et al.* (9); thickness of hydrocarbon region calculated by subtracting 9.0Å (10).

ǂ From Kucerka *et al*. (11).

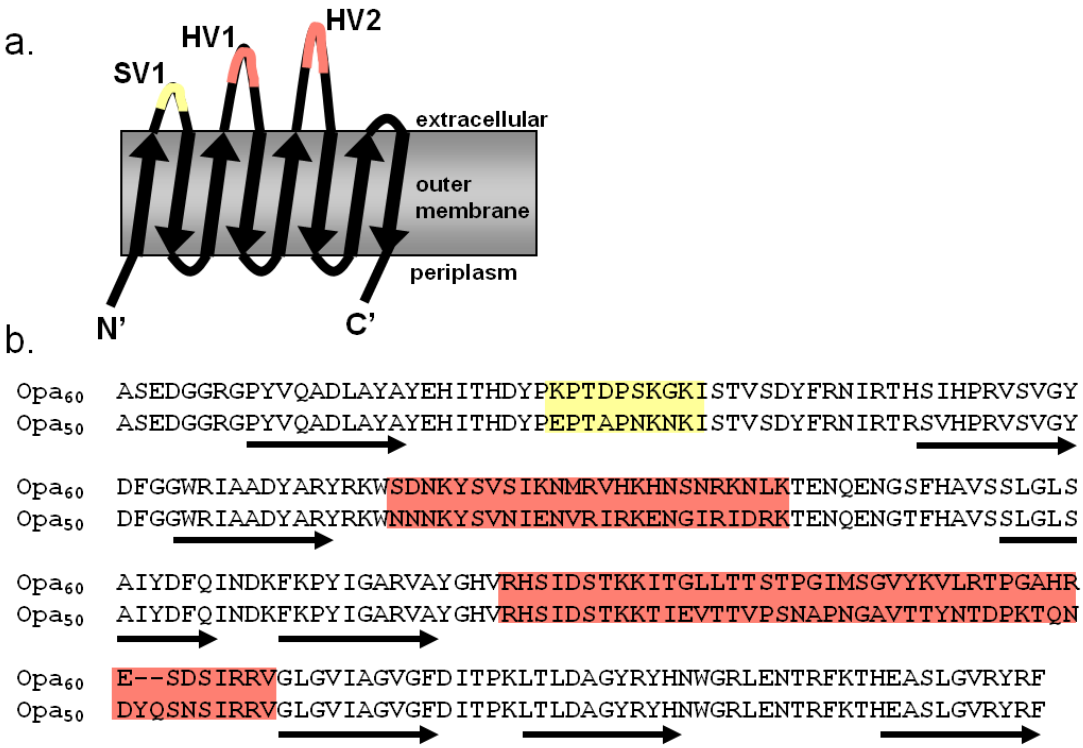

FIGURE S1 Predicted topology of Opa proteins (*a*) and sequence comparison of Opa_{50} and Opa_{60} (*b*). Semivariable loop (SV) is highlighted in yellow and hypervariable loop regions HV1 and HV2 are highlighted in red. Arrows designate predicted β-strands.

Opa_{60} folding in *E. coli* lipid extract

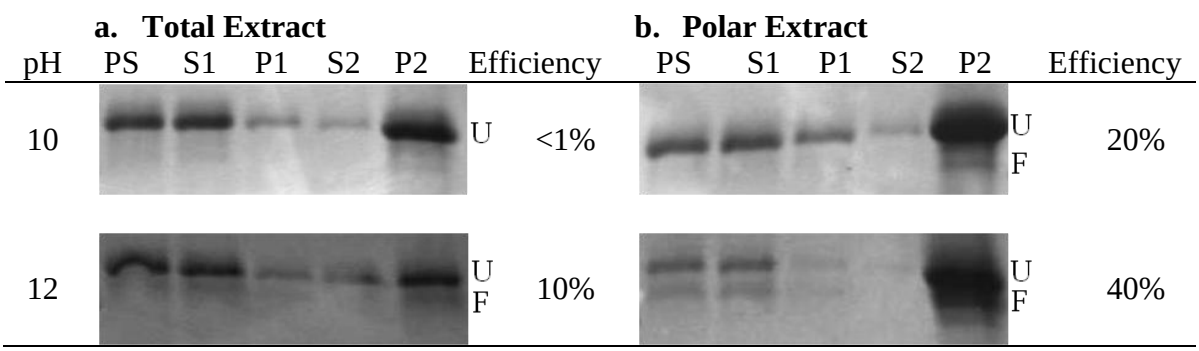

FIGURE S2 Opa_{60} folding in SUVs prepared from native-like *E. coli* (*a*) total lipid extract (57.5% PE, 15.1% PG, 9.8% cardiolipin, and 17.6% of uncharacterized mass) or (*b*) polar extract (67.0% PE, 23.2% PG, 9.8% cardiolipin) at pH 10 or 12. U and F stand for unfolded and folded, respectively. PS, S1, P1, S2, and P2 represent prespin, supernatant 1, pellet 1, supernatant 2, and pellet 2 (see Fig. 2 for details). Overall folding efficiency is low with all *E. coli* lipid extracts, but improves with polar extract at pH 12.

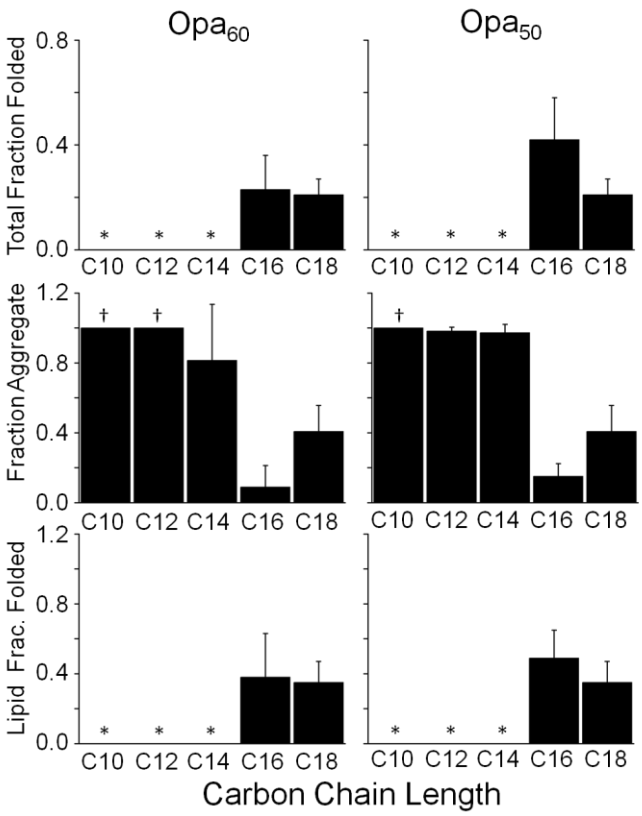

FIGURE S3 Opa_{60} and Opa_{50} folding, aggregation, and lipid insertion vary with lipid carbon chain length at 60 ^{o}C. Opa protein folding in lipid vesicles of saturated phosphocholine with different carbon chain lengths was evaluated following ultracentrifugation and SDS-PAGE with densitometric analysis. All lipids were 2.4 mM in 10 mM sodium borate pH 12 and 1 mM EDTA. The final Opa concentration and molar lipid to protein ratio were 6 µM and 400:1, respectively. For all folding assessments, total fraction folded is the amount of folded protein divided by total protein (lipid-associated + aggregate + folded protein), fraction aggregate is the amount of aggregate divided by total protein, and lipid fraction folded refers to the fraction protein folded of the lipid pellet only (folded / (lipid-associated + folded)). Error bars are standard deviation for at least three separate experiments. For all folding figures, *, folding not observed in at least three separate experiments; †, observed value constant across replicates; ǂ, folding observed in only one of three replicates, deviation not calculated.

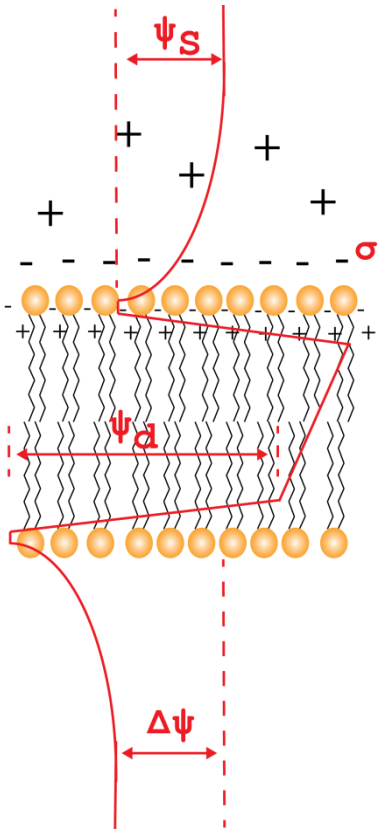

FIGURE S4 Electrical potentials associated with a phospholipid bilayer. The surface potential (only depicted on the top leaflet), Ψ_S, is proportional to the surface charge density (σ) due to charged lipid headgroups at the membrane-solution interface and binding of ions from the bulk solution. The dipole potential, Ψ_D, arises from the alignment of dipolar residues of the lipids and associated water molecules within the membrane. The transmembrane potential, $\Delta\Psi$, results from differences in ion concentration between the two bulk aqueous phases on opposite sides of the bilayer. No transmembrane potential is expected for the vesicles used in this study; and a surface potential is only expected for vesicles containing negatively charged phosphoglycerol (PG) lipids. According to the Gouy-Chapman theory, PG containing vesicles have surface potentials -60 mV, -100 mV, and -140 mV for 10, 25, and 50 mol% PG in phosphocholine vesicles, respectively (12). The dipole potential in phospholipid vesicles is typically ~300 mV, positive relative to the aqueous phase (13, 14).

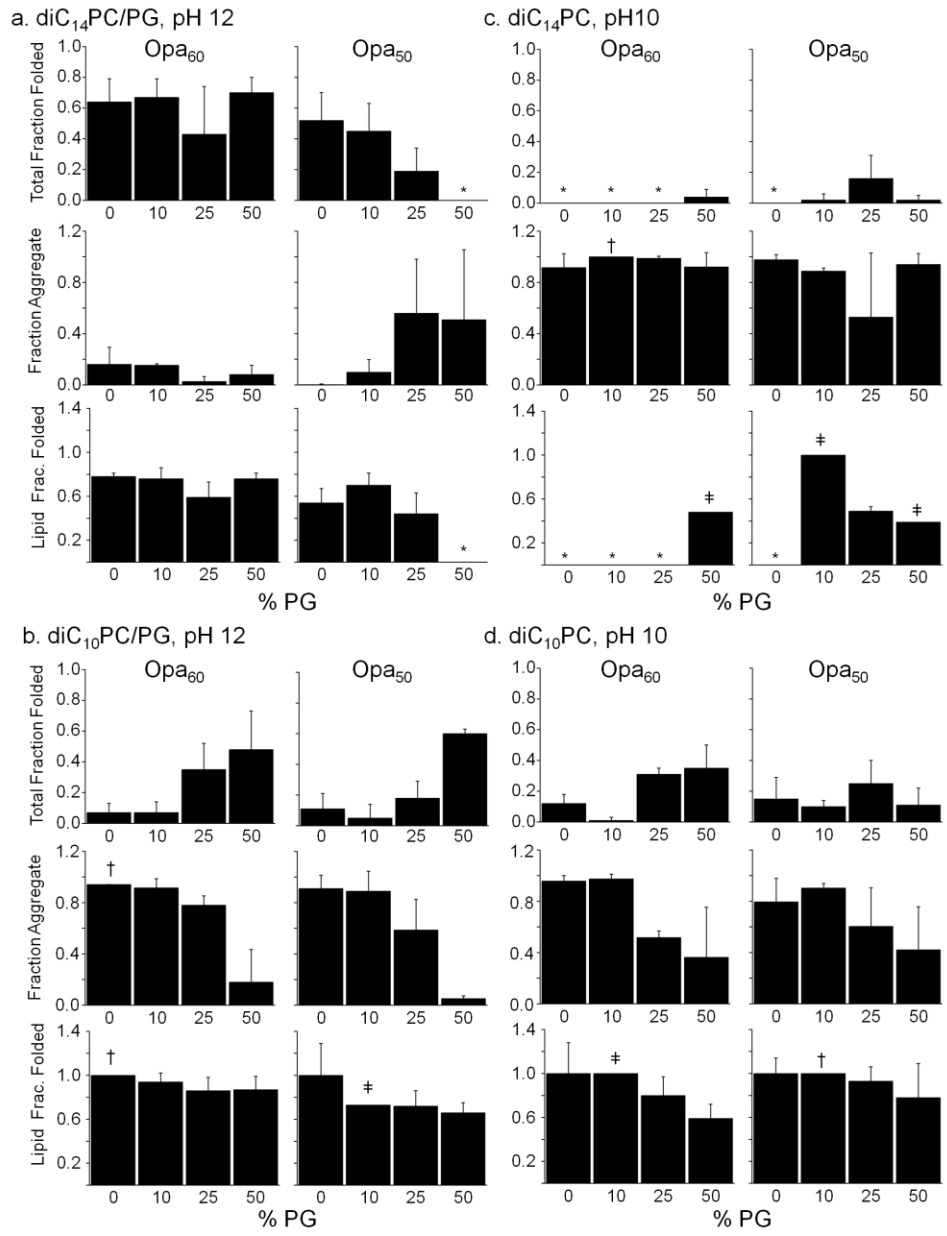

FIGURE S5 Charged lipids impact Opa folding differently in lipid vesicles of $diC_{14}PC$ (*a*) or $diC_{10}PC$ (*b*) at pH 12 and $diC_{14}PC$ (*c*) or $diC_{10}PC$ (*d*) at pH 10. Opa protein folding was assessed following ultracentrifugation and SDS-PAGE with densitometric analysis. All lipids were 2.4 mM in 10 mM sodium borate (pH 12) or 10 mM glycine (pH 10) and 1 mM EDTA. The final Opa concentration and molar lipid to protein ratio were 6 µM and 400:1, respectively. For definitions of fractions and symbols, see Figure S3 legend.

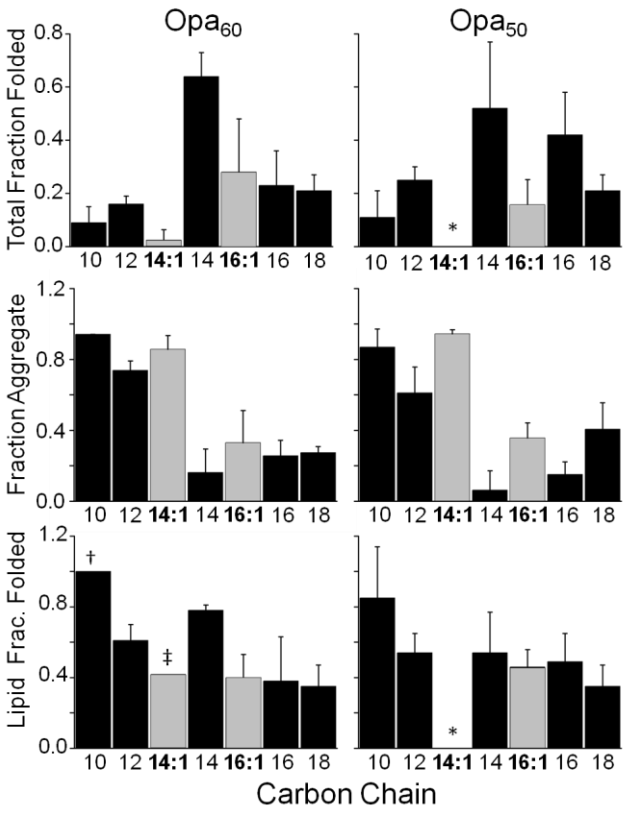

FIGURE S6 Opa protein folding into vesicles of phosphocholine saturated and unsaturated lipids. Opa protein folding was assessed following ultracentrifugation and SDS-PAGE with densitometric analysis. All lipids were 2.4 mM in 10 mM sodium borate pH 12 and 1 mM EDTA. The final Opa concentration and molar lipid to protein ratio were 6 µM and 400:1, respectively. For definitions of fractions and symbols, see Figure S3 legend.

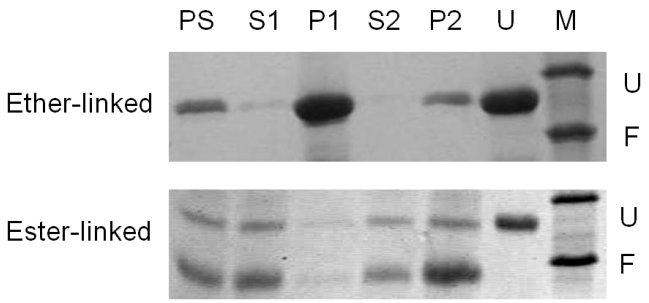

FIGURE S7 Opa_{60} folding in $diC_{14}PC$ phospholipids with ether or ester linkages. Folding is not observed in the ether-linked lipids, which have a smaller internal positive dipole potential than ester-linked phospholipids. PS, S, P designate prespin, supernatant, and pelleted samples, respectively. U and F designate unfolded and folded species. Unfolded control (Opa protein in 8M urea with no lipids) is labeled U; molecular weight marker is labeled M and weights are in kDa

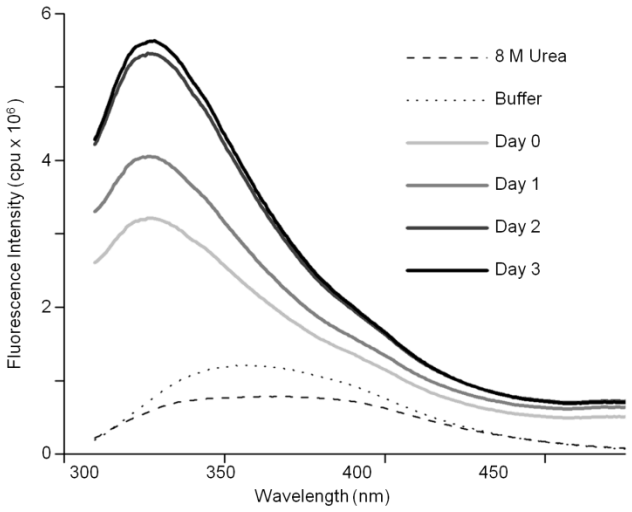

FIGURE S8 Opa_{60} folding in $diC_{14}PC$ liposomes assessed by tryptophan fluorescence. All samples contained 6 µM Opa protein. A blue shift and spike in intensity are seen within mixing time upon the addition of Opa_{60} to lipid vesicles, suggesting that association with the bilayer occurs almost immediately. Fluorescent intensity continues to rise over time as the protein fully inserts and folds into the liposome.

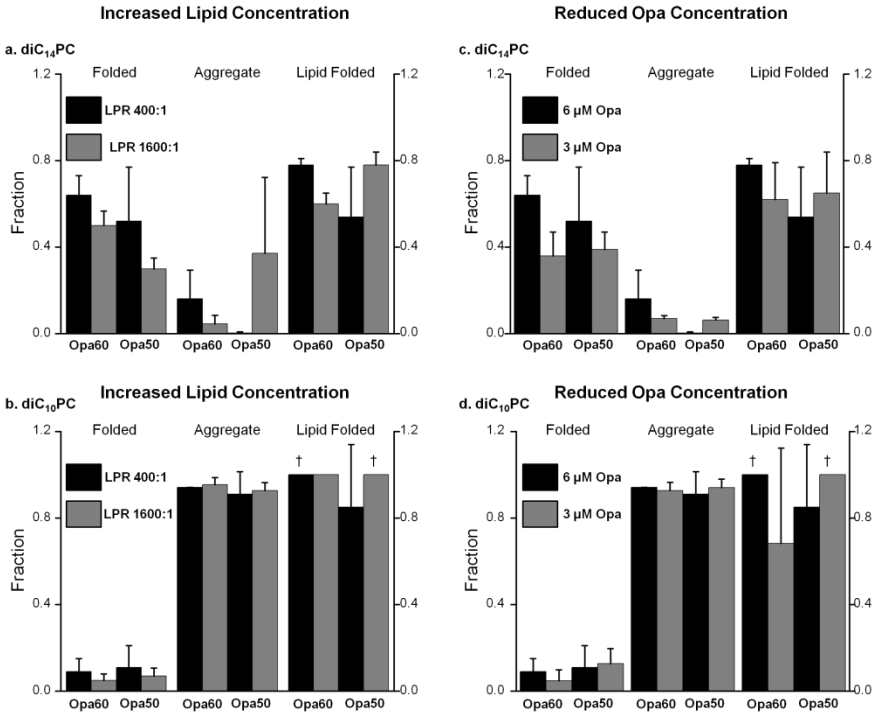

FIGURE S9.The amount of aggregate, lipid-associated, or lipid folded Opa protein did not change when the lipid:protein ratio increased from 400:1 to 1600:1 by using a high concentration of lipids (a,b), or to 800:1 by using a more dilute stock of Opa protein (c,d). Folding was by rapid dilution as described in the text except for variable lipid or protein concentrations as shown in figure. For definitions of fractions and symbols, see Figure S3 legend.

References

1. Kupsch, E. M., B. Knepper, T. Kuroki, I. Heuer, and T. F. Meyer. 1993. Variable opacity (Opa) outer membrane proteins account for the cell tropisms displayed by *Neisseria gonorrhoea*e for human leukocytes and epithelial cells. EMBO J. 12:641-650.
2. Bos, M. P., F. Grunert, and R. J. Belland. 1997. Differential recognition of members of the Carcinoembryonic Antigen family by Opa variants of *Neisseria gonorrhoeae*. Infect Immun 65:2353-2361.
3. ExPaSy Proteomics Server, ProtParam Tool. The Swiss Institute of Bioinformatics.
4. Surrey, T., and F. Jahnig. 1992. Refolding and oriented insertion of a membrane protein into a lipid bilayer. Proc Natl Acad Sci U S A 89:7457-7461.
5. Surrey, T., and F. Jahnig. 1995. Kinetics of folding and membrane insertion of a β-barrel membrane protein. J Biol Chem 270:28199-28203.
6. Kleinschmidt, J. H., and L. K. Tamm. 1996. Folding Intermediates of a β-barrel membrane protein. Kinetic evidence for a multi-step insertion mechanism. Biochemistry 35:12993-13000.
7. Hong, H., and L. K. Tamm. 2004. Elastic coupling of integral membrane protein stability to lipid bilayer forces. Proc Natl Acad Sci U S A 101:4065-4070.
8. Silvius, J. R. 1982. Thermotropic phase transitions of pure lipids in model membranes and their modifications by membrane proteins. John Wiley & Sons, New York.
9. Nagle, J., and S. Tristram-Nagle. 2000. Structure of lipid bilayers. Biochim Biophys Acta 1469:159-195.
10. Lewis, B., and D. Engelman. 1983. Lipid bilayer thickness varies linearly with acyl chain length in fluid phosphatidylcholine vesicles. J Mol Biol 166:211-217.
11. Kucerka, N., J. Gallova, D. Uhrikova, P. Balgavy, M. Bulacu, S. Marrink, and J. Katsaras. 2009. Areas of monounsaturated diacylphosphatidylcholines. Biophys J 97:1926-1932.
12. McLaughlin, S. 1977. Electrostatic potentials at membrane-solution interfaces. In Current topics in membranes and transport. F. Bronner, and A. Kleinzeller, editors. Harcourt Brace Jovanovich, New York. 71-144.
13. Cafiso, D. S. 1995. Influence of charges and dipoles on macromolecular adsorption and permeability. In Permeability and stability of lipid bilayers. E. A. Disalvo, and S. A. Simon, editors. CRC Press, Inc., Boca Raton, Fl. 179-195.
14. Clarke, R. J. 2001. The dipole potential of phospholipid membranes and methods for its detection. Adv Colloid Interface Sci 89:263-281.